Am J Cancer Res 2024;14(3):1139-1156
www.ajcr.us /ISSN:2156-6976/ajcr0154975

Original Article

PU.1 induces tumor-associated macrophages promoting glioma progression through BTK-mediated Akt/mTOR pathway activation

Gu Song[1*], Zeyu Zhang[2*], Yan Chen[3*], Weiliang Hou[4], Weiwei Zhong[5], Yuhang Zhou[3], Anke Zhang[3], Yuanzhi Xu[4,6]

[1]Department of Neurosurgery, The First Affiliated Hospital of Anhui Medical University, Hefei, Anhui, China; [2]Department of Neurosurgery, Renji Hospital, School of Medicine, Shanghai Jiaotong University, Shanghai, China; [3]Department of Neurosurgery, The Second Affiliated Hospital, School of Medicine, Zhejiang University, Hangzhou, Zhejiang, China; [4]Department of Neurosurgery, Huashan Hospital, School of Medicine, Fudan University, Shanghai, China; [5]Department of Anesthesiology, The First Affiliated Hospital of Anhui Medical University, Hefei, Anhui, China; [6]Department of Neurosurgery, Stanford Hospital, Stanford, California, U.S.A. [*]Equal contributors.

Received December 16, 2023; Accepted March 8, 2024; Epub March 15, 2024; Published March 30, 2024

Abstract: Glioma, the most common primary malignant brain tumor, is characterized by infiltrating immune cells that contribute to tumor progression and therapeutic resistance. Tumor-associated macrophages (TAMs) constitute a significant proportion of these infiltrating immune cells and have been implicated in glioma progression. However, the underlying molecular mechanisms by which TAMs promote glioma progression remain elusive. In this study, we investigated the role of PU.1, a crucial transcription factor involved in myeloid cell development, in glioma-associated macrophage polarization and activation. First, bioinformatics and analysis of clinical glioma samples demonstrated a positive correlation between PU.1 expression in TAMs and disease severity. Further experiments using in vitro coculture systems revealed that the expression of PU.1 is increased in glioma cells vs. control cells. Importantly, PU.1-overexpressing macrophages exhibited a protumorigenic phenotype characterized by enhanced migration, invasion, and proliferation. Mechanistically, we found that PU.1-induced activation of the Bruton tyrosine kinase (BTK) signaling pathway led to Akt/mTOR pathway activation in macrophages, which further enhanced their protumorigenic functions. Furthermore, pharmacological inhibition of the BTK or Akt/mTOR pathway reversed the protumorigenic effects of macrophages in vitro and impaired their ability to promote glioma progression in vivo. In conclusion, our study elucidates a novel mechanism by which PU.1 induces the polarization and activation of TAMs in the glioma microenvironment. We highlight the significance of BTK-mediated Akt/mTOR pathway activation in driving the protumorigenic functions of TAMs. Targeting PU.1 and its downstream signaling pathways in TAMs may provide a promising therapeutic strategy to suppress glioma progression and improve patient outcomes.

Keywords: PU.1, tumor-associated macrophages, BTK, Akt, mTOr, glioma

Introduction

Glioma, a common and aggressive type of brain tumor, poses a significant challenge in terms of effective treatment [1]. The tumor microenvironment (TME) plays a critical role in the progression of gliomas, and tumor-associated macrophages (TAMs) are key regulators of this process [2]. TAMs are known to promote tumor growth, invasion, angiogenesis, and immunosuppression [3]. Understanding the molecular mechanisms underlying TAM activation could provide valuable insights for the development of novel therapeutic strategies.

The transcription factor PU.1, a key regulator of myeloid differentiation, has been shown to modulate the polarization and function of macrophages in diverse pathological conditions, including cancer [4, 5]. Its dysregulation has been implicated in promoting tumor progression in various cancer types [6, 7]. Our previous research indicated that PU.1 may be involved in the progression of glioma [8]. However, the role

https://doi.org/10.62347/USAJ2794

of PU.1 in glioma-associated macrophages and its underlying molecular mechanisms remain largely unknown.

Bruton's tyrosine kinase (BTK) has recently emerged as a critical regulator of macrophage polarization and function. The activation of BTK modulates inflammatory responses and downstream signaling cascades [9]. Our previous research suggested that BTK may be a prominent target regulated by PU.1 expression in glioma [8]. Recent research has shown the possible involvement of BTK in the activation of the Akt/mTOR pathway [10]. Moreover, aberrant activation of the Akt/mTOR pathway has been implicated in promoting glioma growth, invasion, and resistance to therapy [11]. Therefore, studies that clarify the interplay between PU.1, TAMs, BTK, and the Akt/mTOR pathway have great potential to reveal novel therapeutic strategies targeting glioma-associated macrophages.

In this study, we aimed to investigate the impact of PU.1 on the induction and polarization of TAMs in the context of glioma. Specifically, we hypothesized that PU.1-mediated activation of TAMs promotes glioma progression through the BTK-mediated Akt/mTOR signaling pathway.

To test our hypothesis, we employed in vitro and in vivo experimental models of glioma. We examined the expression levels of PU.1, BTK, Akt/mTOR signaling components, and TAM-related markers in glioma tissues and TAMs isolated from glioma-bearing mice. We also employed pharmacological and genetic approaches to modulate PU.1, BTK, and Akt/mTOR signaling expression/activity and evaluated the effects of these modulations on TAM polarization and glioma progression.

With this study, we aimed to provide novel insights into the molecular mechanisms underlying TAM activation in glioma and to identify potential therapeutic targets for improving glioma treatment outcomes. Additionally, understanding the role of PU.1 and its interaction with BTK and the Akt/mTOR pathway may have broader implications in the field of cancer immunotherapy.

Methods

Collection of human-derived tumor samples

The sample collection and data analysis were approved by the Institutional Board of Shanghai General Hospital, affiliated with Shanghai Jiao Tong University. Tumor tissues were obtained from the Department of Neurosurgery at Shanghai General Hospital, affiliated with Shanghai Jiao Tong University, between January 2013 and September 2015. The inclusion criteria for patients were as follows: (1) confirmed diagnosis of glioma through histopathological examination and immunohistochemical staining for protein expression (EMP3, Ki67, and PHH3), mutant status (P53, IDH1, and ATRXA), and methylation status of MGMT; and (2) patients undergoing their initial glioma surgery. The exclusion criteria were: (1) patients who had received preoperative radiotherapy or chemotherapy; and (2) patients with uncertain histological grading or staining results for glioma. A total of 81 cases were included in the study.

Data source and expression analysis

Pan-cancer dataset in The Cancer Genome Atlas (TCGA) which consists of 33 kinds of cancer and adjacent tissue samples or GTEx expression matrices was analyzed with an online tool, UCSCXenaShiny (https://hiplot.com.cn/advance/ucsc-xena-shiny) [12]. In this study, we analyzed both glioblastoma multiforme (GBM) and low-grade glioma (LGG). Gliovis (http://gliovis.bioinfo.cnio.es/) was used to get all the expression matrices of gliomas [13]. Publicly available gene-expression datasets of glioma patients (downloaded from NCBI-GEO with accession numbers GSE4290) were also used (http://www.ncbi.nlm.nih.gov/geo/). Statistical analysis for relative gene-expression data were performed using DESeq2 version: v1.4.5. The *P*-values were calculated using the Benjamini and Hochberg method in the R DESeq2 package.

Immune cells and bioinformatic analysis

The single-sample gene set enrichment analysis (ssGSEA) was utilized to determine the enrichment fraction, which represents the absolute enrichment of genomes in each sample within a given dataset. This analysis was

performed using the R package "GSVA" to calculate the normalized enrichment fractions for various types of immune cells. The genome set signatures for 28 immune cells were obtained from a previous study [14]. To assess the immune profile of the glioma samples, Gene Set Variation Analysis (GSVA) from the R package GSVA was employed [8].

Immunohistochemistry

Patient tumor samples and animal tumor tissues were fixed in 4% paraformaldehyde for 24 hours and then embedded in paraffin. Paraffin blocks were cut into 5 μm sections and utilized for hematoxylin and eosin (HE) or immunohistochemistry staining. For immunohistochemistry, rehydrated tissue sections were blocked with goat bovine serum overnight at 4°C and then stained with the following antibodies: PU.1 (catalog ab302623; 1:200; Abcam), CD11c (catalog ab52632; 1:200; Abcam), CD68 (catalog ab125212; 1:200; Abcam), PCNA (catalog ab29; 1:200; Abcam), N-cad (catalog ab76011; 1:200; Abcam), E-cad (catalog ab227639; 1:200; Abcam), and BTK (catalog ab208937; 1:200; Abcam). After washing, the sections were incubated with biotinylated anti-mouse IgG or biotinylated anti-rabbit IgG (obtained from Vector Laboratories, CA, USA). For detection, the ABC method (from Vector Laboratories) was employed, utilizing 3,3' diaminobenzidine (acquired from Dojindo Laboratories, Kumamoto, Japan) as a substrate. The sections were visualized using an AX-80 microscope (manufactured by Olympus, Tokyo, Japan). Subsequently, the images were analyzed using Image J software (available at http://imagej.nih.gov/ij/), and positive expression quantification was performed. Statistical analysis involved the use of Fisher's exact test and Spearman's rank correlation coefficient, considering *P* values below 0.05 as statistically significant.

Cell culture and reagents

U251 cell lines were obtained from the American Type Culture Collection (ATCC) located in Manassas, VA, USA. The U251 cells were cultured in DMEM/F12 medium from Hyclone, UT, USA, supplemented with 2.5% FBS (Invitrogen, CA, USA), 15% horse serum (Invitrogen), and 1% antibiotic mixture. Murine bone marrow-derived macrophages (BMDMs) were obtained from the thigh bone and tibia of C57BL/6 mice through surgical dissection and mechanically separated into single cells by vigorous pipetting. Isolated bone marrow was cultured in RPMI 1640 medium containing 10% FBS, rMCSF (10 ng/mL), and 1% penicillin-streptomycin at 37°C and 5% CO_2. After 3 days, the medium was changed and non-adherent cells were removed.

Migration and invasion assays

To evaluate cell invasion, cells were transfected and incubated for 24 hours. Subsequently, the cells were transferred to serum-free medium for another 12 hours. Upper Transwell chambers were coated with 50 μl of Matrigel (1:8, BD Biosciences) and incubated at 37°C for 30 minutes to allow gel formation. The lower chamber was filled with medium containing 10% fetal bovine serum, while the cell suspension was added to the upper chamber. After 24 hours of incubation at 37°C, the cells were fixed using 4% paraformaldehyde and stained with 0.1% crystal violet. Cell counts were performed in 8 random visual fields. To evaluate migration, the same assay steps were followed, except Matrigel was not used.

CCK-8 assays

CCK-8 assays were conducted to assess cell growth. In brief, 4000 transfected U251 cells were plated in a 96-well plate. The CCK-8 reagent was added at the designated time and incubated for 1 hour at 37°C. The absorbance was measured at 450 nm.

Real-time RT-PCR

Total RNA was extracted from tissue samples and cells using TRIzol reagent (Invitrogen) after washing with PBS. cDNA was synthesized from purified RNA using a SuperScript III First-Strand cDNA synthesis system (18080051, Life Technologies) according to the manufacturer's instructions. SYBR Green PCR Master Mix (Applied Biosystems, CA, USA) was used for PCR amplification and a real-time PCR machine (iQ5, Bio-Rad Laboratories) was used to quantify the expression of mRNAs. β-actin was used as an endogenous control and the expression levels were quantified using 2-ΔΔCt method.

Western blot

Cells and tissues were lysed using RIPA buffer (Beyotime Biotechnology, Beijing, China) containing a protease inhibitor cocktail (B14002, Biotool). The total protein concentration was determined using a bicinchoninic acid protein assay kit (Tiangen Biotech, Beijing, China). Western blotting was performed using primary antibodies against the following targets: β-actin (catalog ab6276; 1:1000; Abcam), phosphorylated Akt (catalog 4060; 1:1000; CST), Akt (catalog 4685; 1:1000; CST), phosphorylated mTOR (catalog 2971; 1:1000; CST), mTOR (catalog 2983; 1:1000; CST), PCNA (catalog 13110; 1:1000; CST), E-cadherin (catalog sc-8426; 1:500; Santa Cruz), N-cadherin (catalog sc-8424; 1:500; Santa Cruz), PU.1 (catalog ab76543; 1:1000; Abcam), Arg1 (catalog ab183333; 1:1000; Abcam), and BTK (catalog ab208937; 1:1000; Abcam). The proteins were separated using 10-12.5% sodium dodecyl sulfate-polyacrylamide gel electrophoresis (SDS-PAGE) and then transferred to polyvinylidene fluoride membranes. To prevent non-specific binding, the membranes were blocked with 5% non-fat milk in TBST (Tris-buffered saline with 0.1% Tween-20). Primary antibodies were incubated with the membranes overnight at 4°C. Afterward, the membranes were washed three times with TBST for 3 minutes each and subsequently incubated with HRP-conjugated IgG secondary antibody at room temperature for 1 hour. Following another round of washing with TBST, the membrane was detected using the Chemi DocXRS + imaging system from Bio-Rad, USA. A supersensitive ECL chemiluminescence kit from Epizyme Biomedical Technology, Shanghai, China, was employed for visualization.

Animal study

The animal manipulations were approved by Animal Core Facility of Shanghai General Hospital, affiliated with Shanghai Jiao Tong University. 1×10^6 U251 cells, which were transfected with luciferase reporter, were suspended in 10 ul of DMEM, and injected into nude mice (female, 6-week-old). The tumor growth was monitored at indicated time. At the end, mice were euthanized by cervical dislocation under anesthesia, and the tumors were fixed and embed using paraffin for further immunohistochemistry analysis.

Lentivirus and transfection

For transfection, BMDMs were inoculated at a density of 40-60% and infected with lentivirus at a multiplicity of infection (MOI) of 20. After 12 h of transfection, the medium was changed. Following cell confluence, the transfected BMDMs were passaged for further experiments. In order to achieve the overexpression and low expression of SPI1, BMDMs were transfected with lentivirus containing LV-SPI1 and LV-shSPI1, respectively (GeneChem Shanghai, China). To avoid off target effects, we used two shSPI1 sequences: shSPI1_1: 5'-AGATGCACGTCCTCGATAC-3'; shSPI1_2: 5'-TCCAGTTCTCGTCCAAGCACAA-3'. Consistent with the results of a previous study [15], these two sequences successfully suppressed the expression of SPI1/PU.1 in BMDMs.

Statistical analysis

Statistical analyses were conducted using SPSS analysis tools (IBM Corp.) or Prism8 software program (GraphPad Software). All data are presented as mean ± standard error of the mean (SEM). To assess statistical significance between two groups, a two-tailed unpaired Student's t-test (for parametric analysis) or Mann-Whitney U test (for non-parametric analysis) was employed. Differences in the results among groups were detected using one-way analysis of variance (ANOVA) followed by Tukey's or Dunnett's multiple comparisons test. A significance level of $P < 0.05$ was considered statistically significant. No sample outliers were excluded.

Results

PU.1 expression associates with glioma progression, especially in TAMs

The transcript levels of SPI1, the gene encoding PU.1, in tumors and adjacent normal tissues were assessed using the UCSCXenaShiny online tool. Pancancer analysis revealed significant differences in SPI1 expression between various tumors and adjacent tissues (**Figure 1A**). Most tumors, including GBM, exhibited higher SPI1 expression than normal tissues ($P < 0.0001$). Notably, there was elevated expression of SPI1 in gliomas with increased malignancy. Analysis of the TCGA, CGGA, and Rembrandt datasets revealed a positive corre-

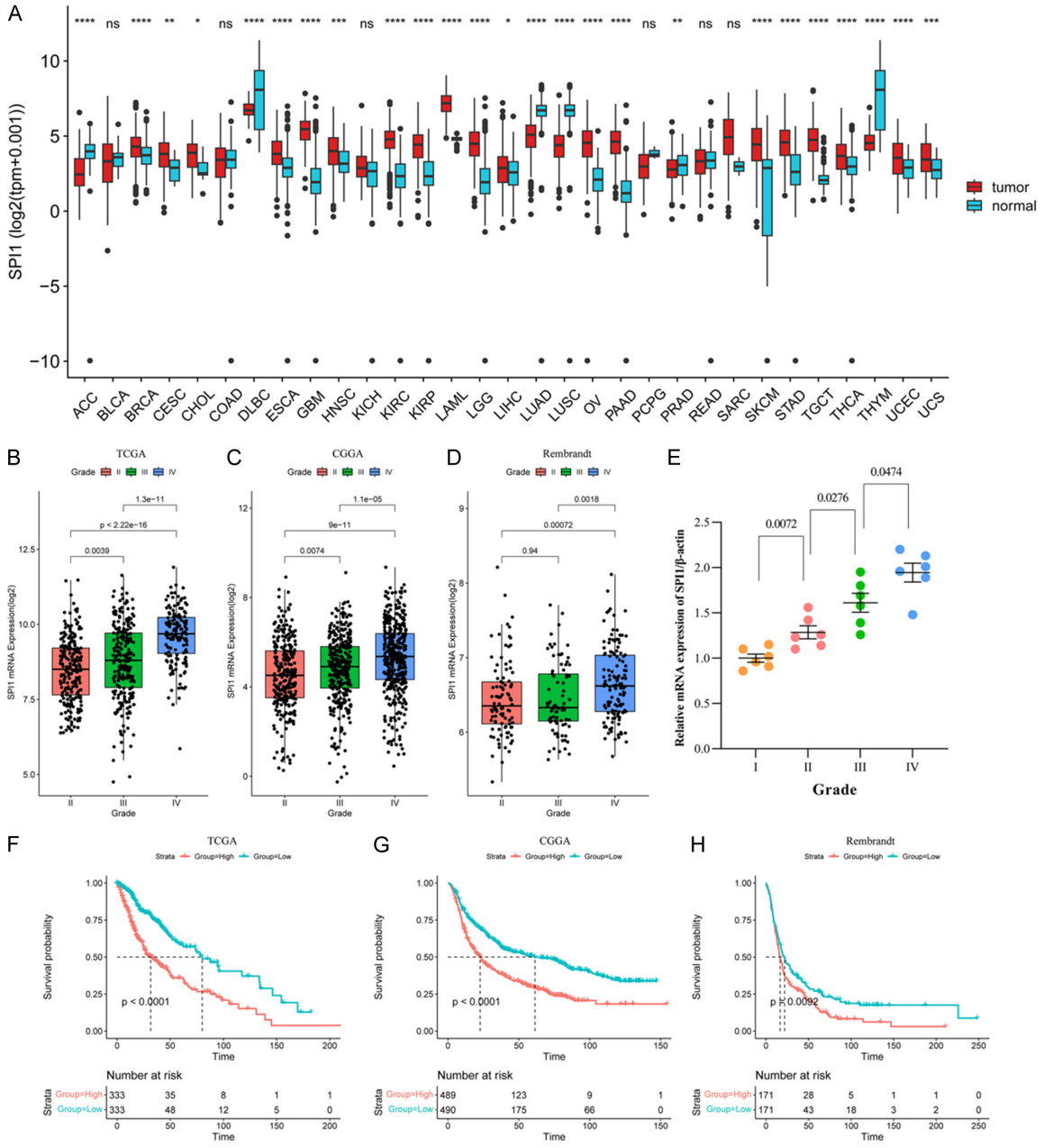

Figure 1. PU.1 expression is associated with glioma progression. (A) UCSCXenaShiny was used to visualize SPI1 mRNA expression in the cancer genome atlas (TCGA) pan-cancer datasets. (B-D) The correlation between SPI1 mRNA expression and glioma grade in TCGA (B), CGGA (C), and Rembrandt (D) database. (E) The correlation between SPI1 mRNA expression and glioma grade in clinical data. (F-H) Survival analysis reveals the impact of SPI1 mRNA expression on the survival of glioma patients in TCGA (F), CGGA (G), and Rembrandt (H) database. *, P < 0.05; **, P < 0.01; ***, P < 0.001; ****, P < 0.0001, ns = no significance.

lation between SPI1 expression levels and glioma grade (**Figure 1B-D**) (P < 0.01). Analysis of our patient cohort corroborated these findings (**Figure 1E**) (P < 0.05). Furthermore, Kaplan-Meier curve analysis demonstrated that patients with high SPI1 expression in the TCGA (P < 0.0001), CGGA (P < 0.0001), and Rembrandt (P < 0.01) datasets had a significantly poorer prognosis than those with low expression (**Figure 1F-H**).

The prognosis of glioma is known to be associated with the infiltration and activation of immune cells [16]. Within the immune microen-

vironment, PU.1 regulates the expression of various genes involved in immune cell signaling, cytokine production, and antigen presentation, thereby influencing communication and coordination among immune cells [7]. Understanding the intricate relationship between PU.1 and the immune microenvironment is essential for developing therapies to modulate immune responses in glioma. To validate these conclusions, we assessed the correlation between SPI1 expression and immune cell infiltration levels. The ssGSEA algorithm was used to systematically estimate the proportions of 28 immune cells from the CGGA dataset (**Figure 2A**). Based on the CGGA and TCGA datasets, Pearson correlation analysis revealed a strong correlation between SPI1 expression and macrophage infiltration levels (**Figure 2B**, **2C**). **Figure 2D** shows the changes in SPI1 expression across different immune cells in various tumors, highlighting a potential association between SPI1 and TAMs. Given the correlation between SPI1 and immune microenvironment features, we used ImmuCellAI to quantify the relative abundances of various tumor-infiltrating immune cells in gliomas (**Figure 2E**). Notably, the proportion of macrophages was significantly different between the high-SPI1 subgroup and low-SPI1 subgroup ($P < 0.0001$). Finally, we analyzed PU.1 expression in our glioma patient cohort and found a positive correlation between PU.1 expression, especially that in CD11c- and CD68-positive cells, and glioma grade (**Figure 2F**) ($P < 0.05$). These findings suggest a potential interplay between PU.1 and TAMs, which may play a pivotal role in glioma progression.

PU.1 regulates TAM polarization to promote glioma progression

To determine whether PU.1 plays a role in TAM-mediated glioma progression, we conducted experiments using murine BMDMs and discovered that overexpressing SPI1 significantly induced the polarization of macrophages toward a tumor-promoting phenotype. This phenotype was characterized by increased expression of Arg1 (**Figure 3A**, **3B**) ($P < 0.05$). To investigate the impact of TAMs on glioma progression, we treated U251 cells with the supernatant of BMDMs. Previous studies have shown that increased expression of PCNA and N-cad, as well as decreased expression of E-cad, suggest tumor progression [17, 18]. Therefore, we assessed the expression of these indicators. The overexpression of SPI1 in BMDMs markedly increased the expression of PCNA and N-cad in U251 cells and decreased the expression of E-cad (**Figure 3C**, **3D**) ($P < 0.05$). Transwell experiments demonstrated that high SPI1 expression in BMDMs promoted the invasion and migration of tumor cells (**Figure 3E**) ($P < 0.05$). Additionally, it also promoted the proliferation of the tumor cells (**Figure 3F**) ($P < 0.05$). Conversely, low SPI1 expression had the opposite effect (all $P < 0.05$).

Next, we conducted animal experiments. SPI1 overexpression significantly promoted tumor growth, as evidenced by increased tumor mass and diameter (**Figure 3G**) ($P < 0.05$). Immunohistochemical staining of the tumor tissue revealed that SPI1 overexpression upregulated the expression of PCNA ($P < 0.05$) and N-cad and downregulated the expression of E-cad, indicating its tumor-promoting effect (**Figure 3H**). Western blot and RT-PCR analyses also showed that SPI1 overexpression led to significant upregulation of Arg1, PCNA, and N-cad, while E-cad was significantly downregulated in the tumor tissue (**Figure 3I**, **3J**) ($P < 0.05$). Conversely, the inhibition of SPI1 expression had the opposite effects (all $P < 0.05$).

These results suggest that PU.1 may promote the progression of glioma by facilitating the polarization of TAMs.

BTK may be involved in PU.1-induced glioma progression

Next, we investigated the potential mechanisms underlying the promotion of glioma by PU.1. In our previous research, we employed an online system for analysis to explore genotype-phenotype associations [8]. Through this analysis, we discovered an association between the SPI1 gene and glioma mediated by the BTK gene. Bruton's agammaglobulinemia tyrosine kinase (BTK) is known for its involvement in X-linked agammaglobulinemia. It has been reported that the BTK gene contains SPI1 binding sites in its promoter region. Notably, in PU.1-/- mice, BTK expression was significantly reduced compared to that in control mice [19]. To further investigate this relationship, we analyzed the changes in the expression of the BTK

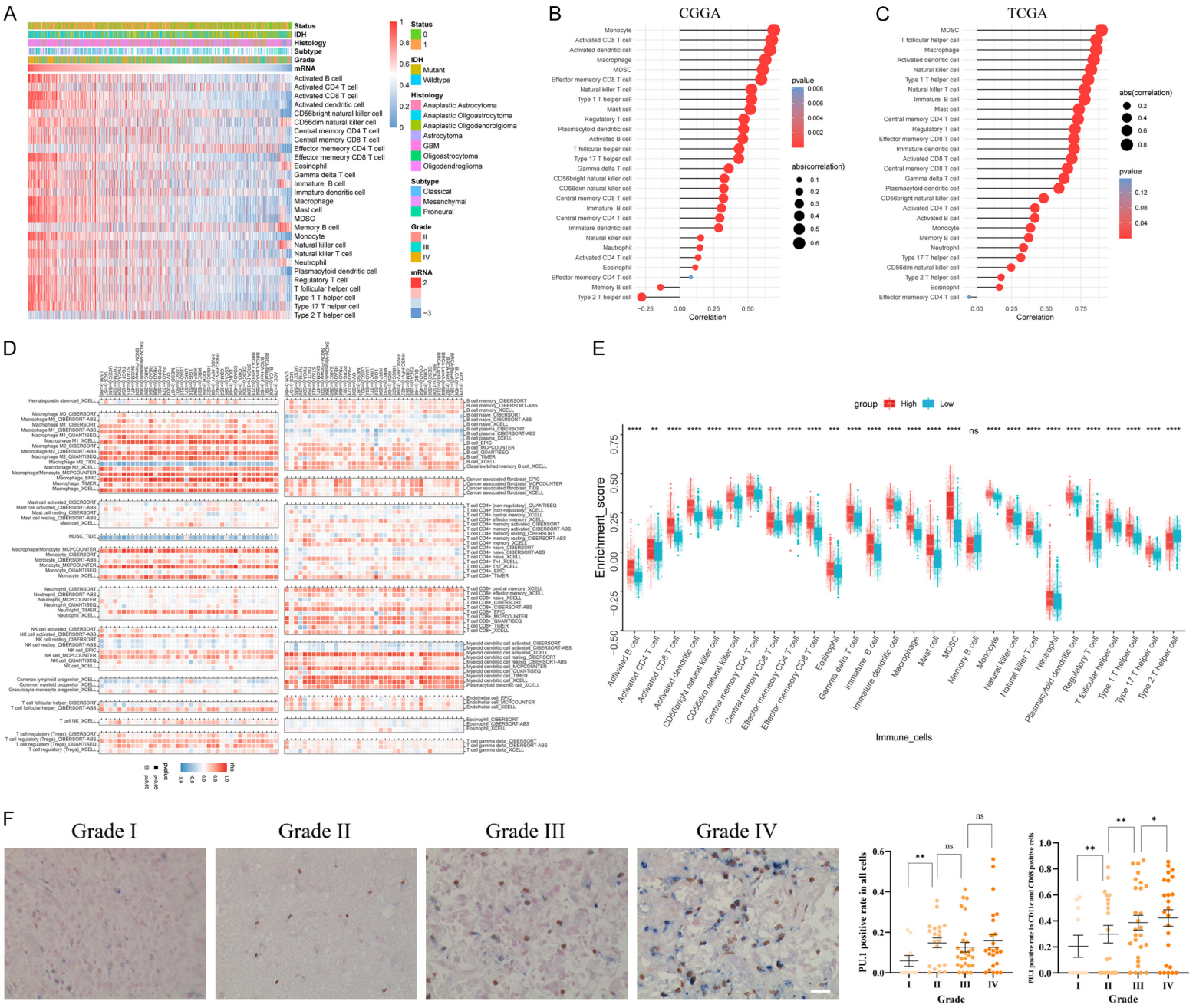
A
Status
IDH
Histology
Subtype
Grade
mRNA
Activated B cell
Activated CD4 T cell
Activated CD8 T cell
Activated dendritic cell
CD56bright natural killer cell
CD56dim natural killer cell
Central memory CD4 T cell
Central memory CD8 T cell
Effector memeory CD4 T cell
Effector memeory CD8 T cell
Eosinophil
Gamma delta T cell
Immature B cell
Immature dendritic cell
Macrophage
Mast cell
MDSC
Memory B cell
Monocyte
Natural killer cell
Natural killer T cell
Neutrophil
Plasmacytoid dendritic cell
Regulatory T cell
T follicular helper cell
Type 1 T helper cell
Type 17 T helper cell
Type 2 T helper cell
Mutant
Wildtype
Anaplastic Astrocytoma
Anaplastic Oligoastrocytoma
Anaplastic Oligodendrolgioma
Astrocytoma
GBM
Oligoastrocytoma
Oligodendroglioma
Classical
Mesenchymal
Proneural
II
III
IV
B
CGGA
pvalue
abs(correlation)
Correlation
C
TCGA
abs(correlation)
pvalue
Correlation
D
pval
padj
pvalue
rho
E
group
High
Low
Enrichment_score
Immune_cells
F
Grade I
Grade II
Grade III
Grade IV
PU.1 positive rate in all cells
PU.1 positive rate in CD11c and CD68 positive cells
Grade

Figure 2. Analysis of the immune microenvironment of PU.1 in gliomas. (A) Heatmap showing SPI1-associated relative abundance of immune cells in gliomas, annotations show corresponding clinical features of each sample. (B, C) The correlation between the ssGSEA scores of immune cells and the expression of SPI1 in gliomas based on CGGA (B) and TCGA (C) database. (D) Changes in SPI1 expression in different immune cells in various tumors. SPI1 expression varies among different types of macrophages in various tumors. (E) ImmuCellAI quantifies the relative abundances of various tumor-infiltrating immune cells in gliomas. Proportion of tumor-infiltrating macrophages is significantly different between SPI1 high and low subgroups. (F) Immunohistochemistry of clinical glioma samples to evaluate the association between PU.1 expression and glioma grade (bar = 20 μm). *, P < 0.05; **, P < 0.01; ***, P < 0.001; ****, P < 0.0001, ns = no significance.

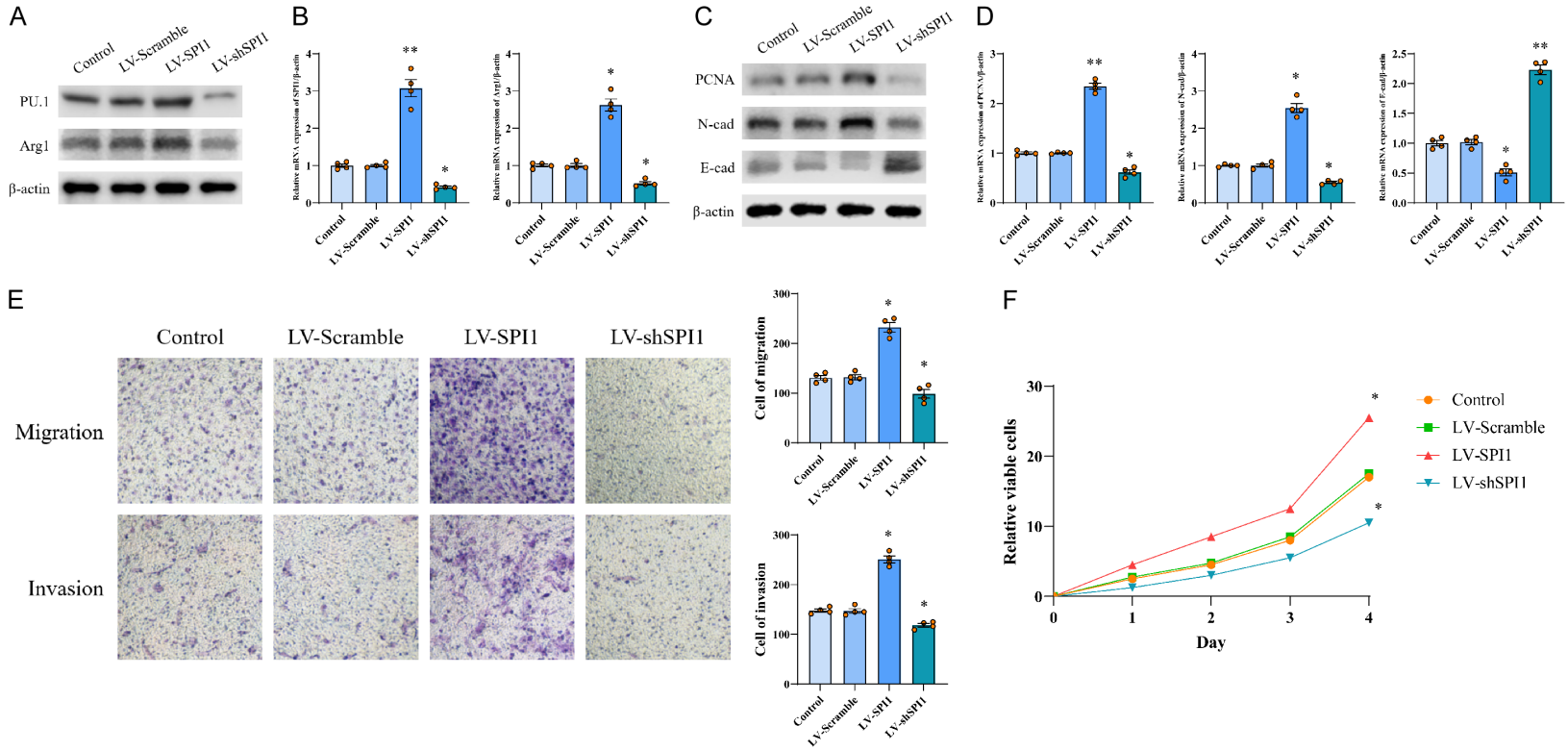

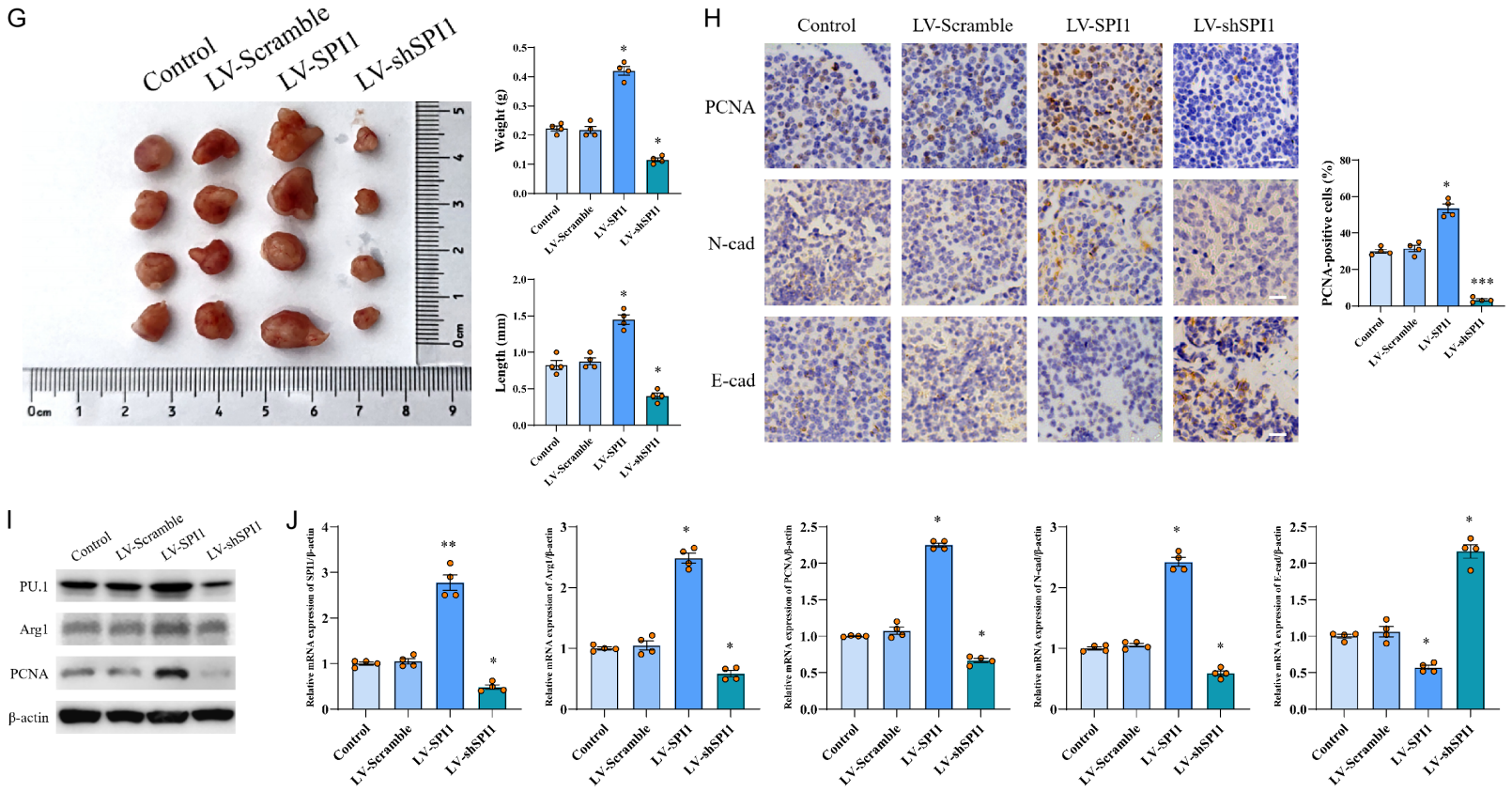

Figure 3. PU.1 promotes glioma progression by regulating TAM polarization. (A, B) Protein (A) and mRNA (B) expression of PU.1 and Arg1 (of groups Control, LV-Scramble, LV-SPI1, and LV-shSPI1; the same below) in BMDMs. (C, D) Protein (C) and mRNA (D) expression of PCNA, N-cad, and E-cad in U251 cells. (E) Transwell experiment evaluates the migration and invasion ability of tumor cells. (F) CCK 8 experiment evaluates the proliferation ability of tumor cells. (G) Representative images showing tumors harvested from mice bearing tumors. (H) Immunohistochemistry was used to evaluate the expression of PCNA, N-cad, and E-cad in the tumor tissue (bar = 20 μm). (I, J) Protein (I) and mRNA (J) expression of PU.1, Arg1, PCNA, N-cad, and E-cad in the tumor tissue. *, $P < 0.05$; **, $P < 0.01$; ***, $P < 0.001$; ****, $P < 0.0001$, ns = no significance, compared with the group LV-Scramble.

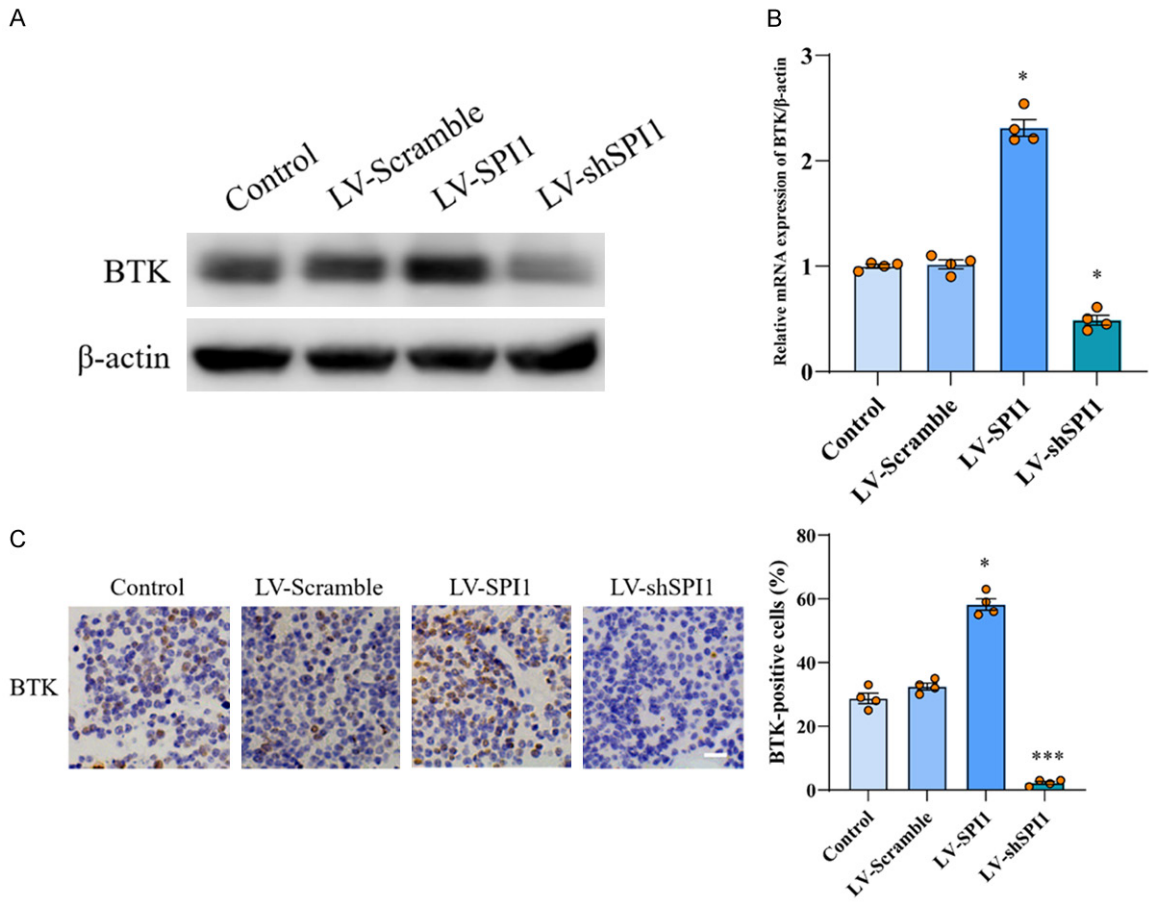

Figure 4. PU.1 promotes BTK expression in glioma. (A, B) Protein (A) and mRNA (B) expression of BTK (of groups Control, LV-Scramble, LV-SPI1, and LV-shSPI1; the same below) in BMDMs. (C) Immunohistochemistry was used to evaluate the expression of BTK in the tumor tissue (bar = 20 μm). *, P < 0.05; **, P < 0.01; ***, P < 0.001; ****, P < 0.0001, ns = no significance, compared with the group LV-Scramble.

gene using glioma RNA array data, which were also utilized for SPI1 expression analysis. Figure S1A, S1B illustrates our findings, highlighting a noteworthy increase in BTK mRNA expression within the glioma dataset (quoted from our previous study) [8]. Further cellular and animal experiments showed that overexpression of SPI1 significantly increased the expression of BTK in BMDMs and tumor tissues, while low expression of SPI1 decreased the expression of BTK (**Figure 4A-C**) (P < 0.05). These findings suggest that BTK is likely an important factor involved in the role of PU.1 in TAM polarization and glioma progression.

BTK inhibition rescued PU.1-mediated TAM polarization and glioma progression

To determine whether BTK plays a role in PU.1-mediated TAM polarization and glioma progression, we conducted experiments using BMDMs and discovered that the BTK inhibitor ibrutinib significantly attenuated the increase in Arg1 expression induced by SPI1 overexpression (**Figure 5A**, **5B**) (P < 0.05). Next, we treated U251 cells with the supernatant of BMDMs and found that the treatment BMDMs with ibrutinib reversed the changes in the expression of PCNA, N-cad, and E-cad induced by SPI1 overexpression in U251 cells (**Figure 5C**, **5D**) (P < 0.05). In addition, Transwell and CCK-8 experiments showed that ibrutinib treatment of BMDMs significantly inhibited SPI1 overexpression-induced U251 cell proliferation, invasion, and migration (**Figure 5E**, **5F**) (P < 0.05).

Animal experiments showed that ibrutinib rescued SPI1 overexpression-induced tumor growth, as indicated by decreases in tumor

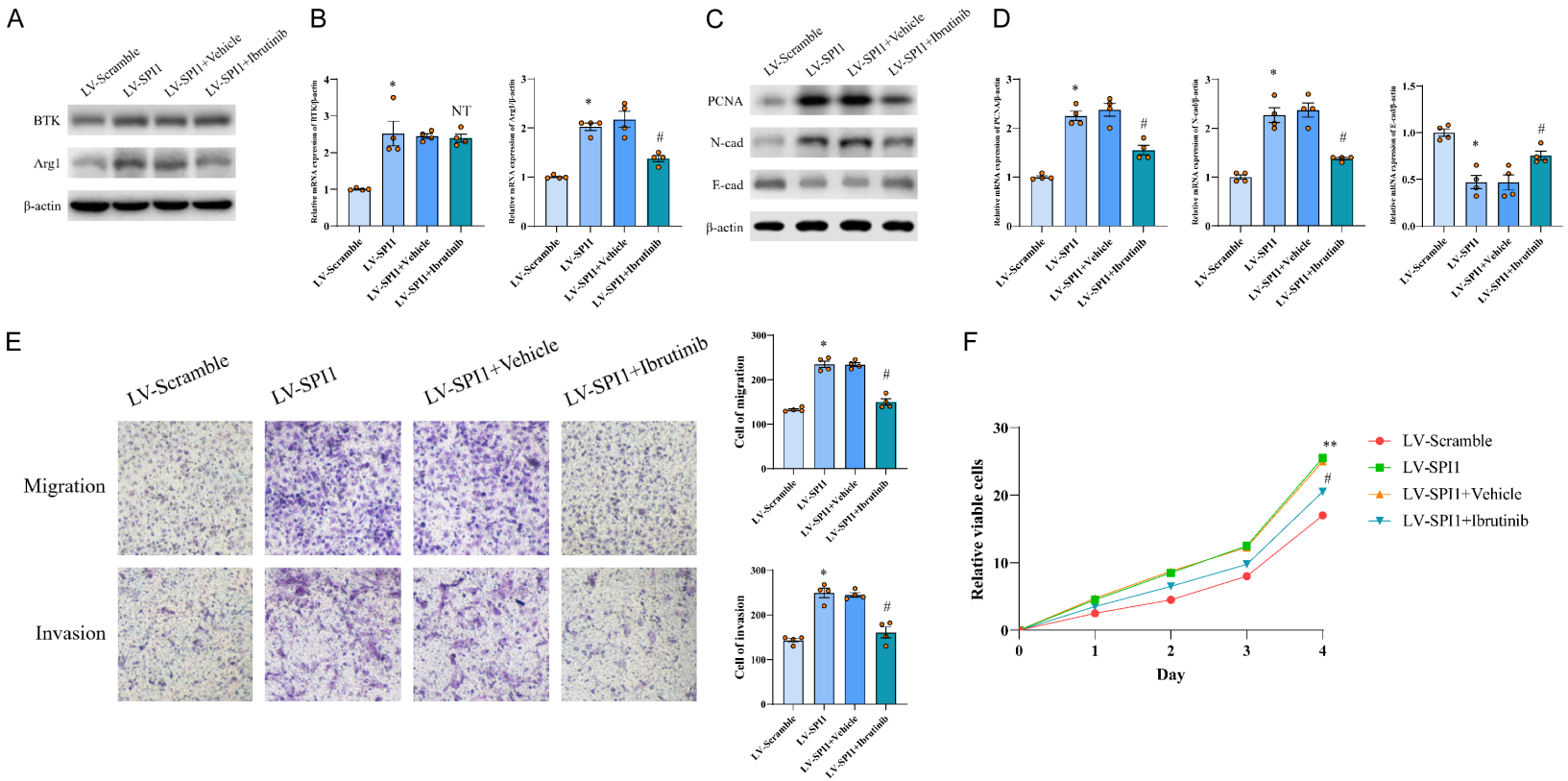
A
LV-Scramble
LV-SPI1
LV-SPI1+Vehicle
LV-SPI1+Ibrutinib
BTK
Arg1
β-actin
B
NT
C
PCNA
N-cad
E-cad
β-actin
D
E
Migration
Invasion
Cell of migration
Cell of invasion
F
Relative viable cells
Day
LV-Scramble
LV-SPI1
LV-SPI1+Vehicle
LV-SPI1+Ibrutinib

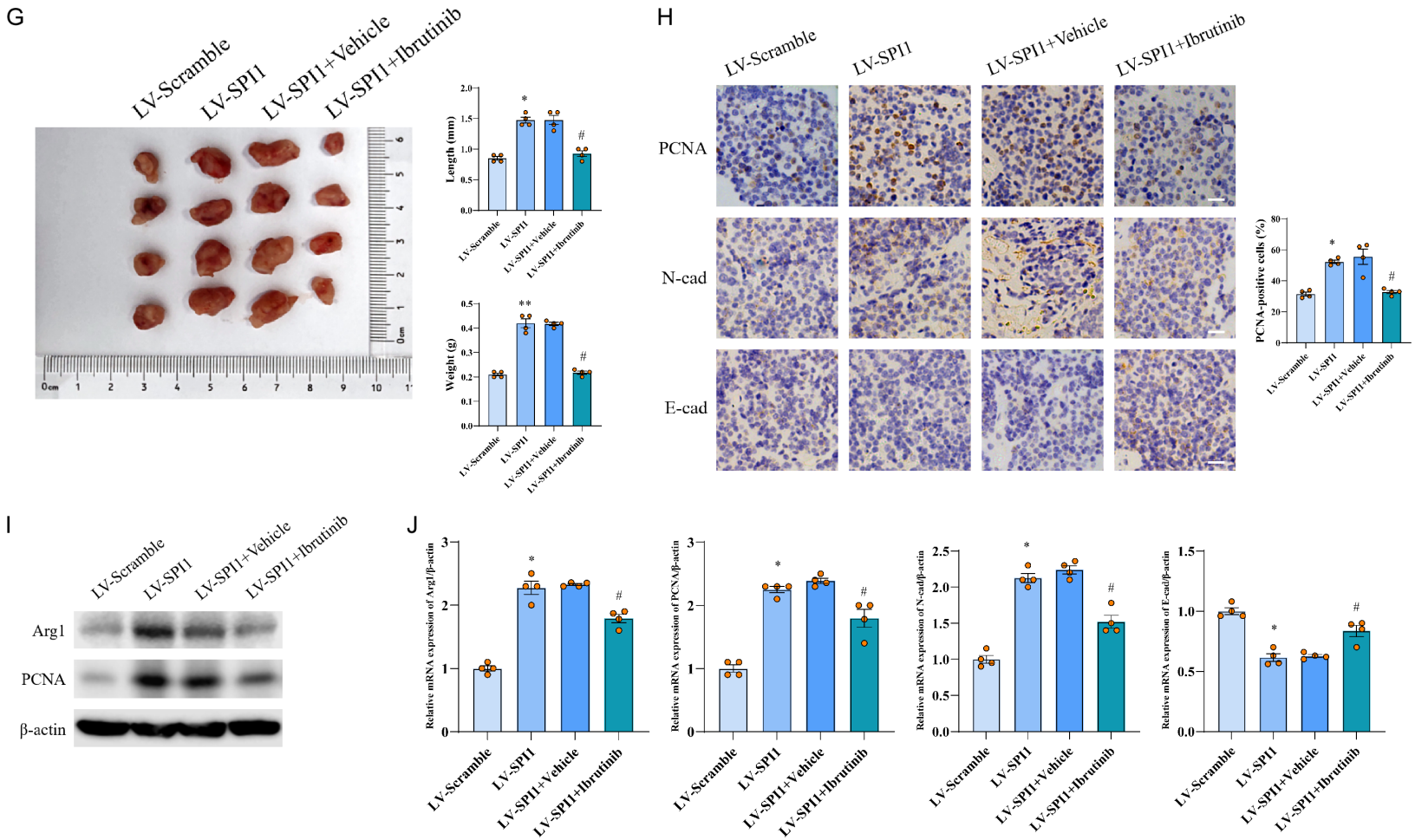

Figure 5. BTK inhibition reverses PU.1-mediated TAM polarization and glioma progression. (A, B) Protein (A) and mRNA (B) expression of BTK and Arg1 (of groups LV-Scramble, LV-SPI1, LV-SPI1+Vehicle, and LV-SPI1+Ibrutinib; the same below) in BMDMs. (C, D) Protein (C) and mRNA (D) expression of PCNA, N-cad, and E-cad in U251 cells. (E) Transwell experiment evaluates the migration and invasion ability of tumor cells. (F) CCK 8 experiment evaluates the proliferation ability of tumor cells. (G) Representative images showing tumors harvested from mice bearing tumors. (H) Immunohistochemistry was used to evaluate the expression of PCNA, N-cad, and E-cad in the tumor tissue (bar = 20 μm). (I, J) Protein (I) and mRNA (J) expression of Arg1, PCNA, N-cad, and E-cad in the tumor tissue. *, $P < 0.05$; **, $P < 0.01$; ***, $P < 0.001$; ****, $P < 0.0001$, ns = no significance, compared with the group of LV-Scramble; #, $P < 0.05$; ##, $P < 0.01$; ###, $P < 0.001$; ####, $P < 0.0001$, ns = no significance, compared with the group of LV-SPI1+Vehicle.

mass and diameter (**Figure 5G**) ($P < 0.05$). Immunohistochemical staining of SPI1-overexpressing tumor tissue revealed that ibrutinib downregulated the expression of PCNA ($P < 0.05$) and N-cad and upregulated the expression of E-cad (**Figure 5H**). Western blot and RT-PCR analyses also showed that ibrutinib treatment significantly decreased Arg1, PCNA, and N-cad expression and significantly increased E-cad expression in the tumor tissue (**Figure 5I**, **5J**) ($P < 0.05$).

In addition, ibrutinib treatment inhibited the polarization of TAMs into the tumor-promoting phenotype and thus inhibited the progression of glioma (Figure S2A-F).

These results indicate that PU.1 may promote TAM polarization and glioma progression through BTK.

BTK mediates PU.1-induced TAM polarization and glioma progression through Akt/mTOR pathway

The Akt/mTOR signaling pathway is a key regulator of cell survival, growth, and metabolism. Recent studies have highlighted the significance of Akt/mTOR activation in TAM polarization and function [11]. Furthermore, research has demonstrated the involvement of BTK in the activation of the Akt/mTOR pathway [10]. Hence, we explored the role of Akt/mTOR in PU.1/BTK-mediated TAM polarization and the progression of glioma. First, we observed that SPI1 promoted the activation of the Akt/mTOR pathway in BMDMs, whereas ibrutinib treatment reversed this effect (**Figure 6A**). Next, we found that the increase in Arg1 expression induced by SPI1 overexpression was significantly attenuated in cells treated with the mTOR inhibitor rapamycin (**Figure 6B**, **6C**) ($P < 0.05$). We further treated U251 cells with the supernatant of BMDMs and found that rapamycin treatment of BMDMs reversed the changes in the expression of PCNA, N-cad, and E-cad induced by SPI1 overexpression in U251 cells (**Figure 6D**, **6E**) ($P < 0.05$). Additionally, Transwell and CCK-8 experiments demonstrated that rapamycin treatment of BMDMs significantly inhibited the SPI1 overexpression-induced proliferation, invasion, and migration of U251 cells (**Figure 6F**, **6G**) ($P < 0.05$).

Animal experiments demonstrated that rapamycin effectively rescued SPI1 overexpression-induced tumor growth. This rescue effect was highlighted by a reduction in tumor mass and diameter, as depicted in **Figure 6H** ($P < 0.05$). Immunohistochemical staining of SPI1-overexpressing tumor tissue revealed that rapamycin significantly decreased the expression of PCNA ($P < 0.05$) and N-cad while concurrently increasing the expression of E-cad, as displayed in **Figure 6I**. Further analysis via Western blotting and RT-PCR confirmed that treatment with rapamycin resulted in notable downregulation of Arg1, PCNA, and N-cad in the tumor tissue, while E-cad expression was significantly upregulated, as shown in **Figure 6J**, **6K** ($P < 0.05$).

In addition, rapamycin treatment inhibited the polarization of TAMs into the tumor-promoting phenotype and thus inhibited the progression of glioma (Figure S3A-F).

These results suggest that BTK may promote PU.1-induced TAM polarization and glioblastoma progression by activating the Akt/mTOR pathway.

Discussion

Gliomas, one of the most aggressive and prevalent forms of brain tumors, pose a significant challenge in the field of oncology due to their complex biology, invasiveness, and resistance to conventional therapies [1]. The intricacy of the TME in gliomas, especially concerning the role of immune cells, such as TAMs, in tumor progression, is an area of active investigation [2]. TAMs, a major component of the TME, contribute to various aspects of tumorigenesis, including immune suppression, angiogenesis, and tumor cell invasion [3]. Hence, exploring the molecular mechanisms guiding TAM polarization and function is of utmost importance in the development of innovative therapeutic strategies for gliomas. In this study, we elucidated a previously unidentified mechanism whereby the transcription factor PU.1 activates the Akt/mTOR signaling pathway via BTK, inducing TAM polarization and consequently promoting glioma progression.

PU.1, an Ets family transcription factor, is instrumental in the development and differentiation of hematopoietic cells [20]. It regulates

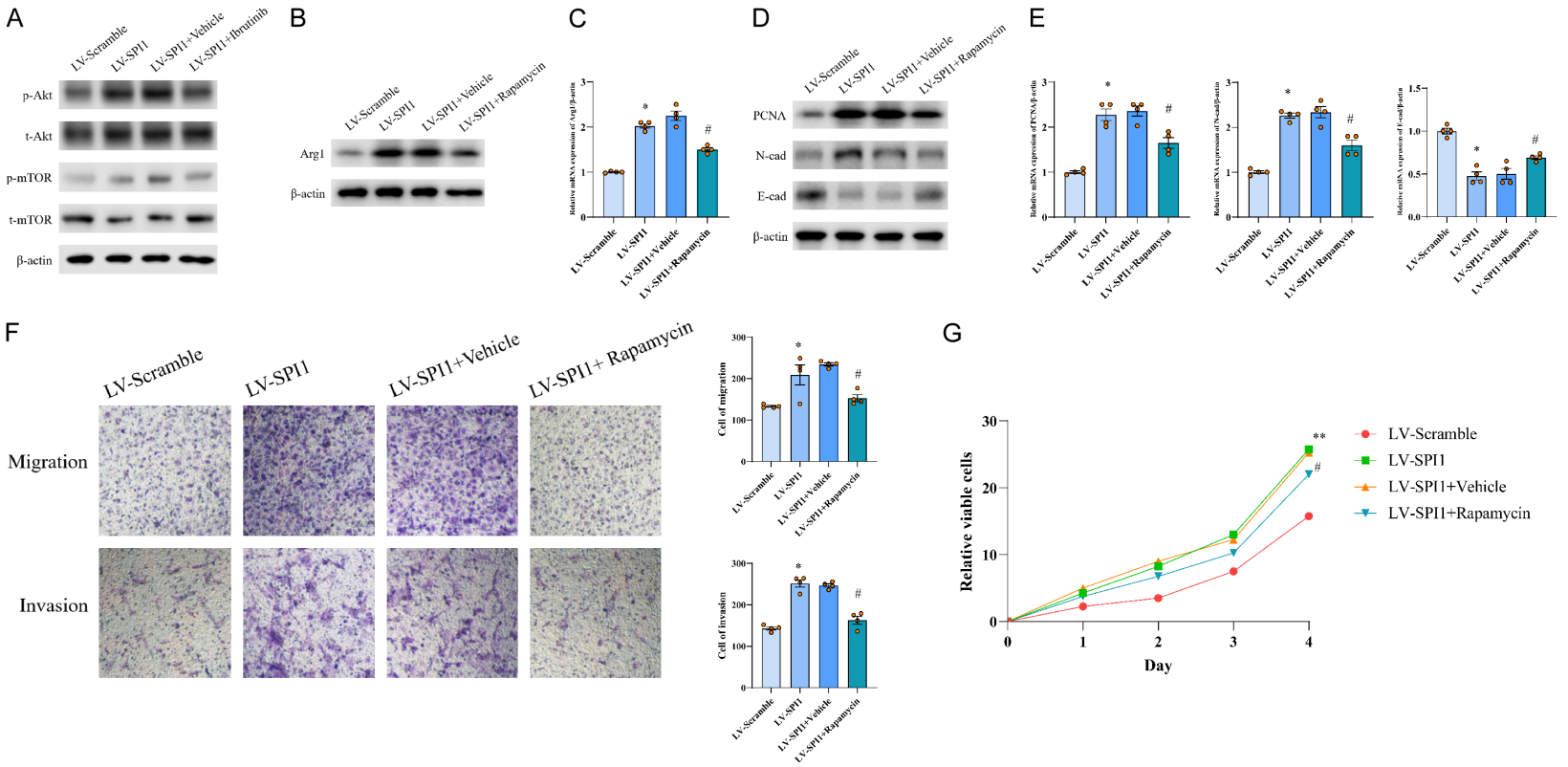
A
LV-Scramble
LV-SPI1
LV-SPI1+Vehicle
LV-SPI1+Ibrutinib
p-Akt
t-Akt
p-mTOR
t-mTOR
β-actin
B
LV-Scramble
LV-SPI1
LV-SPI1+Vehicle
LV-SPI1+Rapamycin
Arg1
β-actin
C
D
LV-Scramble
LV-SPI1
LV-SPI1+Vehicle
LV-SPI1+Rapamycin
PCNA
N-cad
E-cad
β-actin
E
F
LV-Scramble
LV-SPI1
LV-SPI1+Vehicle
LV-SPI1+ Rapamycin
Migration
Invasion
Cell of migration
Cell of invasion
G
Relative viable cells
Day
LV-Scramble
LV-SPI1
LV-SPI1+Vehicle
LV-SPI1+Rapamycin

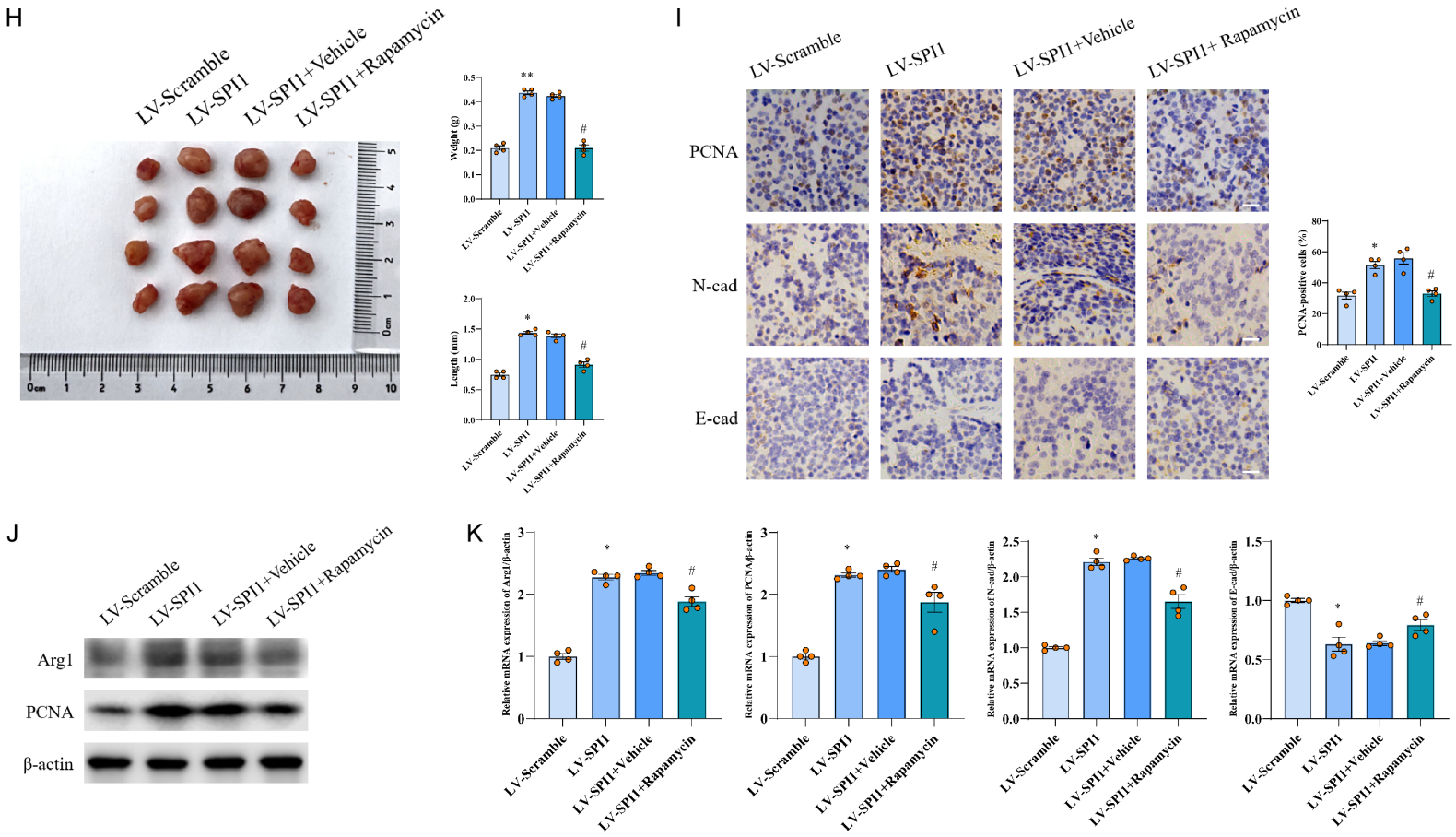

Figure 6. BTK activates Akt/mTOR pathway to mediate PU.1-induced TAM polarization and glioma progression. (A) Protein expression of phosphorylated Akt, Akt, phosphorylated mTOR, and mTOR (of groups LV-Scramble, LV-SPI1, LV-SPI1+Vehicle, and LV-SPI1+Ibrutinib) in BMDMs. (B, C) Protein (B) and mRNA (C) expression of Arg1 (of groups LV-Scramble, LV-SPI1, LV-SPI1+Vehicle, and LV-SPI1+Rapamycin; the same below) in BMDMs. (D, E) Protein (D) and mRNA (E) expression of PCNA, N-cad, and E-cad in U251 cells. (F) Transwell experiment evaluates the migration and invasion ability of tumor cells. (G) CCK 8 experiment evaluates the proliferation ability of tumor cells. (H) Representative images showing tumors harvested from mice bearing tumors. (I) Immunohistochemistry was used to evaluate the expression of PCNA, N-cad, and E-cad in the tumor tissue (bar = 20 μm). (J, K) Protein (J) and mRNA (K) expression of Arg1, PCNA, N-cad, and E-cad in the tumor tissue. *, P < 0.05; **, P < 0.01; ***, P < 0.001; ****, P < 0.0001, ns = no significance, compared with the group of LV-Scramble; #, P < 0.05; ##, P < 0.01; ###, P < 0.001; ####, P < 0.0001, ns = no significance, compared with the group of LV-SPI1+Vehicle.

the expression of a myriad of genes implicated in immune cell signaling, antigen presentation, and cytokine production [21]. Our research expands the existing knowledge by demonstrating the crucial role of PU.1 in regulating TAM polarization within the glioma microenvironment. We revealed that overexpression of PU.1 resulted in the transcriptional activation and expression of BTK in the glioma TME. BTK, a nonreceptor tyrosine kinase, modulates multiple signaling pathways associated with cell survival, proliferation, and migration [9]. Our findings indicate that PU.1-mediated BTK upregulation subsequently activates the Akt/mTOR signaling pathway, a key regulator of cellular growth and survival. This activation culminates in the promotion of TAM polarization, which promotes a protumoral phenotype characterized by glioma cell proliferation, invasion, and migration. Therefore, SPI1/PU.1 expression ratio may be an important biomarker for predicting the prognosis of glioma patients.

The engagement of the Akt/mTOR pathway in TAM regulation and its influence on glioma progression have profound therapeutic implications [22-25]. Our data suggest that targeting the PU.1/BTK/Akt/mTOR axis may constitute a novel approach for inhibiting TAM-driven glioma progression. We demonstrated that inhibiting BTK activity markedly decreased Akt/mTOR pathway activation, subsequently reducing TAM polarization and glioma progression. This observation suggested that BTK targeting, and consequently targeting the Akt/mTOR pathway, could be a viable strategy for inhibiting TAM-driven glioma progression. Furthermore, our study elucidates the complex interplay between PU.1 and the glioma immune microenvironment, emphasizing the necessity of modulating the immune response, specifically by targeting TAM polarization and function, as a critical component of efficacious glioma therapy.

Several limitations of our study warrant further investigation. Primarily, our study is largely centered on in vitro and cell line-based molecular mechanisms, necessitating the validation of these findings in in vivo animal models of glioma. Additionally, the potential off-target effects of BTK inhibition and its repercussions on other immune cells within the TME require comprehensive evaluation. Moreover, the clinical efficacy of targeting the PU.1/BTK/Akt/mTOR axis should be assessed in clinical trials to ascertain its feasibility as a therapeutic strategy for glioma patients.

In conclusion, our study revealed a novel mechanism by which PU.1 facilitates glioma progression by activating the BTK/Akt/mTOR signaling axis, leading to the polarization of TAMs toward a protumoral phenotype. Targeting this axis may represent a promising therapeutic avenue for gliomas. However, further research is needed to validate these findings in preclinical models of glioma and to assess the feasibility of integrating this approach into existing therapeutic strategies for glioma. Ultimately, a thorough understanding of the molecular mechanisms governing TAM polarization and function will be essential for developing more effective and targeted therapies for glioma.

Overall, our research provides novel insights into the molecular mechanisms underlying glioma progression and highlights the potential therapeutic implications of targeting the PU.1/BTK/Akt/mTOR axis. The findings of this study reveal new avenues for further research and may contribute to the development of innovative therapeutic strategies for glioma patients.

Conclusions

In summary, our study revealed a novel regulatory mechanism in which the transcription factor PU.1 activates the Akt/mTOR signaling pathway via BTK to induce the polarization of TAMs toward a protumoral phenotype, thereby promoting glioma progression. We showed that PU.1 triggers the transcriptional activation of BTK, which in turn activates the Akt/mTOR pathway, promoting TAM polarization and glioma cell proliferation and migration. Importantly, our data indicate that inhibiting BTK activity significantly suppresses Akt/mTOR pathway activation, TAM polarization, and glioma progression. These findings reveal the pivotal role of the PU.1/BTK/Akt/mTOR axis in the regulation of TAM polarization and glioma progression, highlighting the therapeutic potential of targeting this axis for glioma treatment. Further research is warranted to explore the therapeutic efficacy of BTK inhibitors and to assess the feasibility of integrating this approach into existing therapeutic strategies for glioma. In addition, our findings also suggest that the

SPI1 expression/PU.1 ratio may serve as an important biomarker for predicting the prognosis of glioma patients. Ultimately, a comprehensive understanding of the molecular mechanisms governing TAM polarization and function will be essential for developing more effective and targeted therapies for glioma.

Acknowledgements

This study is supported by Shanghai Pujiang Talent Program (22PJD009).

Disclosure of conflict of interest

None.

Address correspondence to: Anke Zhang, Department of Neurosurgery, The Second Affiliated Hospital, School of Medicine, Zhejiang University, Hangzhou, Zhejiang, China. E-mail: theanke@163.com; Yuanzhi Xu, Department of Neurosurgery, Huashan Hospital, School of Medicine, Fudan University, Shanghai, China. E-mail: juliusxu@stanford.edu

References

[1] Xu S, Tang L, Li X, Fan F and Liu Z. Immunotherapy for glioma: current management and future application. Cancer Lett 2020; 476: 1-12.

[2] Peng P, Zhu H, Liu D, Chen Z, Zhang X, Guo Z, Dong M, Wan L, Zhang P, Liu G, Zhang S, Dong F, Hu F, Cheng F, Huang S, Guo D, Zhang B, Yu X and Wan F. TGFBI secreted by tumor-associated macrophages promotes glioblastoma stem cell-driven tumor growth via integrin αvβ5-Src-Stat3 signaling. Theranostics 2022; 12: 4221-4236.

[3] Fu LQ, Du WL, Cai MH, Yao JY, Zhao YY and Mou XZ. The roles of tumor-associated macrophages in tumor angiogenesis and metastasis. Cell Immunol 2020; 353: 104119.

[4] Shen C, Chen MT, Zhang XH, Yin XL, Ning HM, Su R, Lin HS, Song L, Wang F, Ma YN, Zhao HL, Yu J and Zhang JW. The PU.1-modulated microRNA-22 is a regulator of monocyte/macrophage differentiation and acute myeloid leukemia. PLoS Genet 2016; 12: e1006259.

[5] Ha SD, Cho W, DeKoter RP and Kim SO. The transcription factor PU.1 mediates enhancer-promoter looping that is required for IL-1β eRNA and mRNA transcription in mouse melanoma and macrophage cell lines. J Biol Chem 2019; 294: 17487-17500.

[6] Wang L, Wang E, Prado Balcazar J, Wu Z, Xiang K, Wang Y, Huang Q, Negrete M, Chen KY, Li W, Fu Y, Dohlman A, Mines R, Zhang L, Kobayashi Y, Chen T, Shi G, Shen JP, Kopetz S, Tata PR, Moreno V, Gersbach C, Crawford G, Hsu D, Huang E, Bu P and Shen X. Chromatin remodeling of colorectal cancer liver metastasis is mediated by an HGF-PU.1-DPP4 axis. Adv Sci (Weinh) 2021; 8: e2004673.

[7] Kastner P and Chan S. PU.1: a crucial and versatile player in hematopoiesis and leukemia. Int J Biochem Cell Biol 2008; 40: 22-27.

[8] Xu Y, Gu S, Bi Y, Qi X, Yan Y and Lou M. Transcription factor PU.1 is involved in the progression of glioma. Oncol Lett 2018; 15: 3753-3759.

[9] McDonald C, Xanthopoulos C and Kostareli E. The role of Bruton's tyrosine kinase in the immune system and disease. Immunology 2021; 164: 722-736.

[10] Jin L, Mo Y, Yue EL, Liu Y and Liu KY. Ibrutinib ameliorates cerebral ischemia/reperfusion injury through autophagy activation and PI3K/Akt/mTOR signaling pathway in diabetic mice. Bioengineered 2021; 12: 7432-7445.

[11] Mohamed E, Kumar A, Zhang Y, Wang AS, Chen K, Lim Y, Shai A, Taylor JW, Clarke J, Hilz S, Berger MS, Solomon DA, Costello JF, Molinaro AM and Phillips JJ. PI3K/AKT/mTOR signaling pathway activity in IDH-mutant diffuse glioma and clinical implications. Neuro Oncol 2022; 24: 1471-1481.

[12] Wang S, Xiong Y, Zhao L, Gu K, Li Y, Zhao F, Li J, Wang M, Wang H, Tao Z, Wu T, Zheng Y, Li X and Liu XS. UCSCXenaShiny: an R/CRAN package for interactive analysis of UCSC Xena data. Bioinformatics 2022; 38: 527-529.

[13] Bowman RL, Wang Q, Carro A, Verhaak RG and Squatrito M. GlioVis data portal for visualization and analysis of brain tumor expression datasets. Neuro Oncol 2017; 19: 139-141.

[14] Hänzelmann S, Castelo R and Guinney J. GSVA: gene set variation analysis for microarray and RNA-seq data. BMC Bioinformatics 2013; 14: 7.

[15] Antony-Debré I, Paul A, Leite J, Mitchell K, Kim HM, Carvajal LA, Todorova TI, Huang K, Kumar A, Farahat AA, Bartholdy B, Narayanagari SR, Chen J, Ambesi-Impiombato A, Ferrando AA, Mantzaris I, Gavathiotis E, Verma A, Will B, Boykin DW, Wilson WD, Poon GM and Steidl U. Pharmacological inhibition of the transcription factor PU.1 in leukemia. J Clin Invest 2017; 127: 4297-4313.

[16] Grabowski MM, Sankey EW, Ryan KJ, Chongsathidkiet P, Lorrey SJ, Wilkinson DS and Fecci PE. Immune suppression in gliomas. J Neurooncol 2021; 151: 3-12.

[17] Liao S, Chen H, Liu M, Gan L, Li C, Zhang W, Lv L and Mei Z. Aquaporin 9 inhibits growth and metastasis of hepatocellular carcinoma cells

via Wnt/β-catenin pathway. Aging (Albany NY) 2020; 12: 1527-1544.
[18] Zhang A, Xu Y, Xu H, Ren J, Meng T, Ni Y, Zhu Q, Zhang WB, Pan YB, Jin J, Bi Y, Wu ZB, Lin S and Lou M. Lactate-induced M2 polarization of tumor-associated macrophages promotes the invasion of pituitary adenoma by secreting CCL17. Theranostics 2021; 11: 3839-3852.
[19] Müller S, Sideras P, Smith CI and Xanthopoulos KG. Cell specific expression of human Bruton's agammaglobulinemia tyrosine kinase gene (Btk) is regulated by Sp1- and Spi-1/PU.1-family members. Oncogene 1996; 13: 1955-1964.
[20] Li G, Hao W and Hu W. Transcription factor PU.1 and immune cell differentiation (Review). Int J Mol Med 2020; 46: 1943-1950.
[21] Oikawa T, Yamada T, Kihara-Negishi F, Yamamoto H, Kondoh N, Hitomi Y and Hashimoto Y. The role of Ets family transcription factor PU.1 in hematopoietic cell differentiation, proliferation and apoptosis. Cell Death Differ 1999; 6: 599-608.
[22] Liu X, Zhao P, Wang X, Wang L, Zhu Y, Song Y and Gao W. Celastrol mediates autophagy and apoptosis via the ROS/JNK and Akt/mTOR signaling pathways in glioma cells. J Exp Clin Cancer Res 2019; 38: 184.
[23] Jin Q, Zhao J, Zhao Z, Zhang S, Sun Z, Shi Y, Yan H, Wang Y, Liu L and Zhao Z. CAMK1D inhibits glioma through the PI3K/AKT/mTOR signaling pathway. Front Oncol 2022; 12: 845036.
[24] Li X, Wu C, Chen N, Gu H, Yen A, Cao L, Wang E and Wang L. PI3K/Akt/mTOR signaling pathway and targeted therapy for glioblastoma. Oncotarget 2016; 7: 33440-33450.
[25] Barzegar Behrooz A, Talaie Z, Jusheghani F, Łos MJ, Klonisch T and Ghavami S. Wnt and PI3K/Akt/mTOR survival pathways as therapeutic targets in glioblastoma. Int J Mol Sci 2022; 23: 1353.

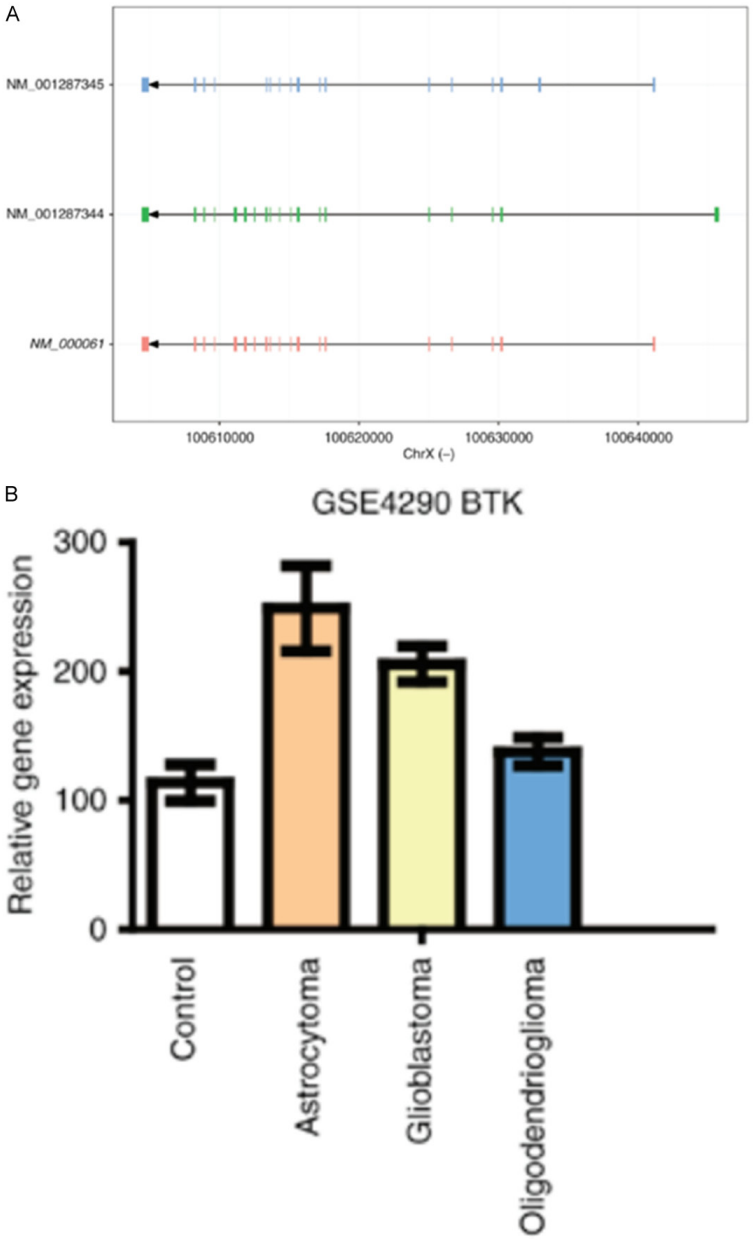

Figure S1. BTK may be a target for PU.1 induced glioma progression. A. Gene locus for BTK transcription at the genome. Transcript in italic was analyzed in the study. Arrows, direction of transcription. Box, exons in indicated genes. Each line indicated one transcript for the corresponding gene. B. Fold changes of BTK expression levels in three types of glioma samples. Database used was as indicated.

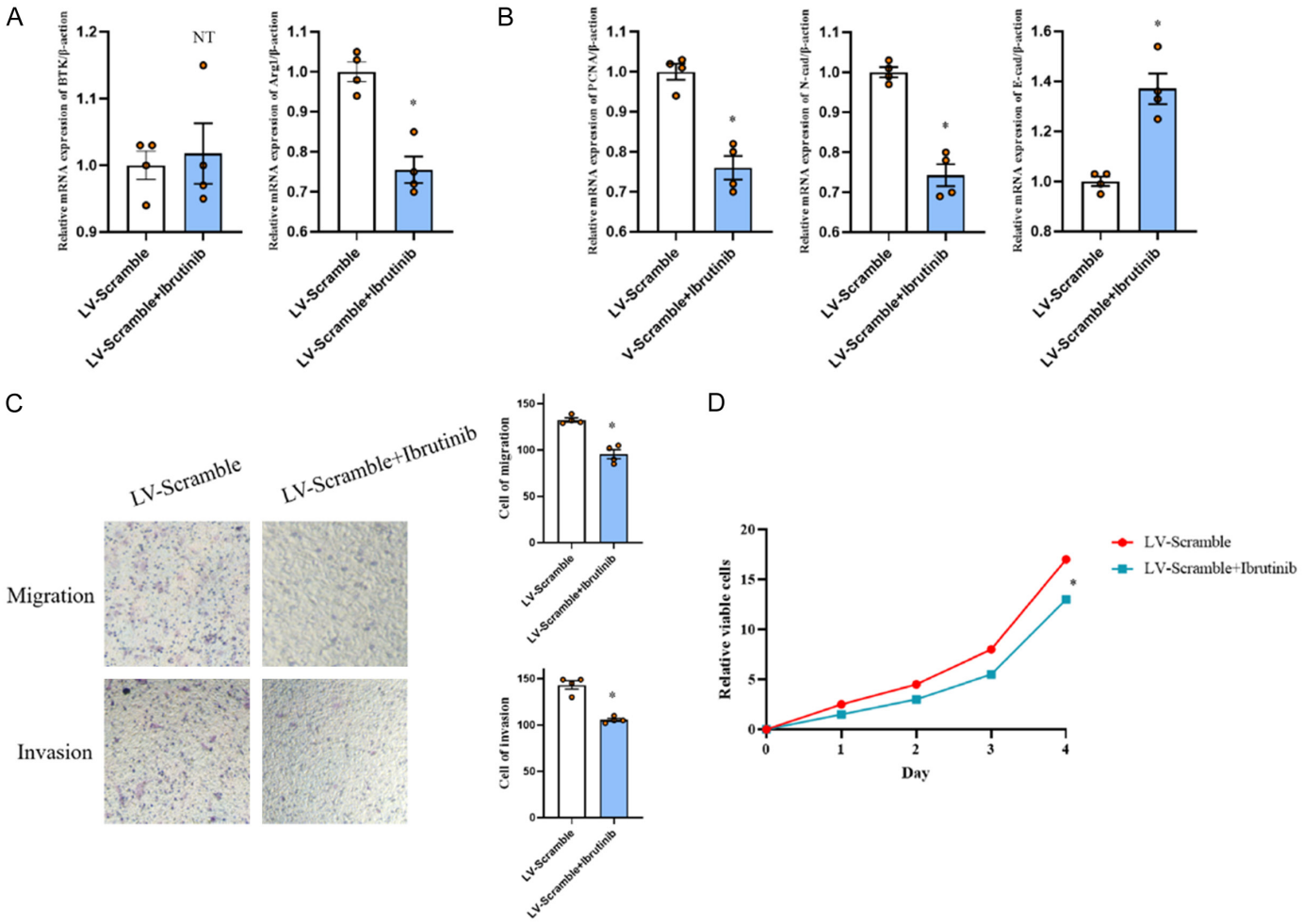
A
Relative mRNA expression of BTK/β-action
NT
LV-Scramble
LV-Scramble+Ibrutinib
Relative mRNA expression of Arg1/β-action
B
Relative mRNA expression of PCNA/β-action
V-Scramble+Ibrutinib
Relative mRNA expression of N-cad/β-action
Relative mRNA expression of E-cad/β-action
C
LV-Scramble
LV-Scramble+Ibrutinib
Migration
Invasion
Cell of migration
Cell of invasion
D
Relative viable cells
Day
LV-Scramble
LV-Scramble+Ibrutinib

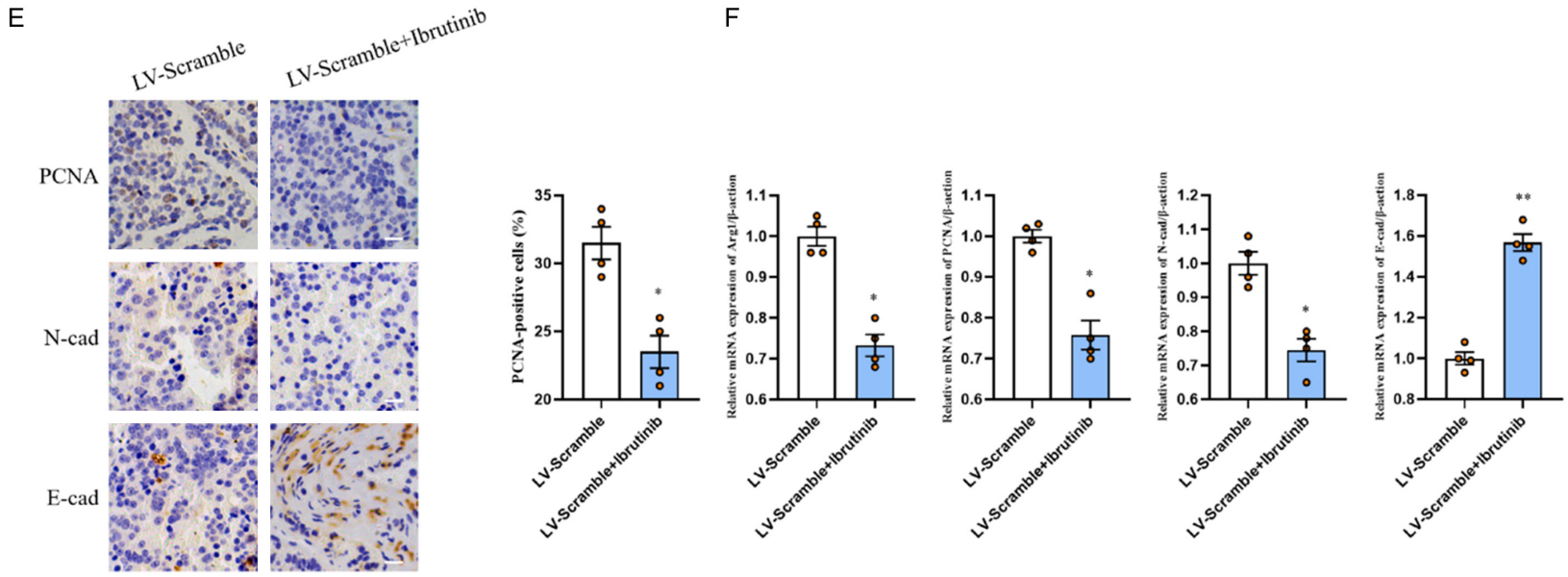

Figure S2. Ibrutinib inhibits TAM polarization and glioma progression. A. mRNA expression of BTK and Arg1 (of groups LV-Scramble and LV-Scramble+Ibrutinib; the same below) in BMDMs. B. mRNA expression of PCNA, N-cad, and E-cad in U251 cells. C. Transwell experiment evaluates the migration and invasion ability of tumor cells. D. CCK 8 experiment evaluates the proliferation ability of tumor cells. E. Immunohistochemistry was used to evaluate the expression of PCNA, N-cad, and E-cad in the tumor tissue (bar = 20 μm). F. mRNA expression of Arg1, PCNA, N-cad, and E-cad in the tumor tissue. *, P < 0.05; **, P < 0.01; ***, P < 0.001; ****, P < 0.0001, ns = no significance, compared with the group of LV-Scramble.

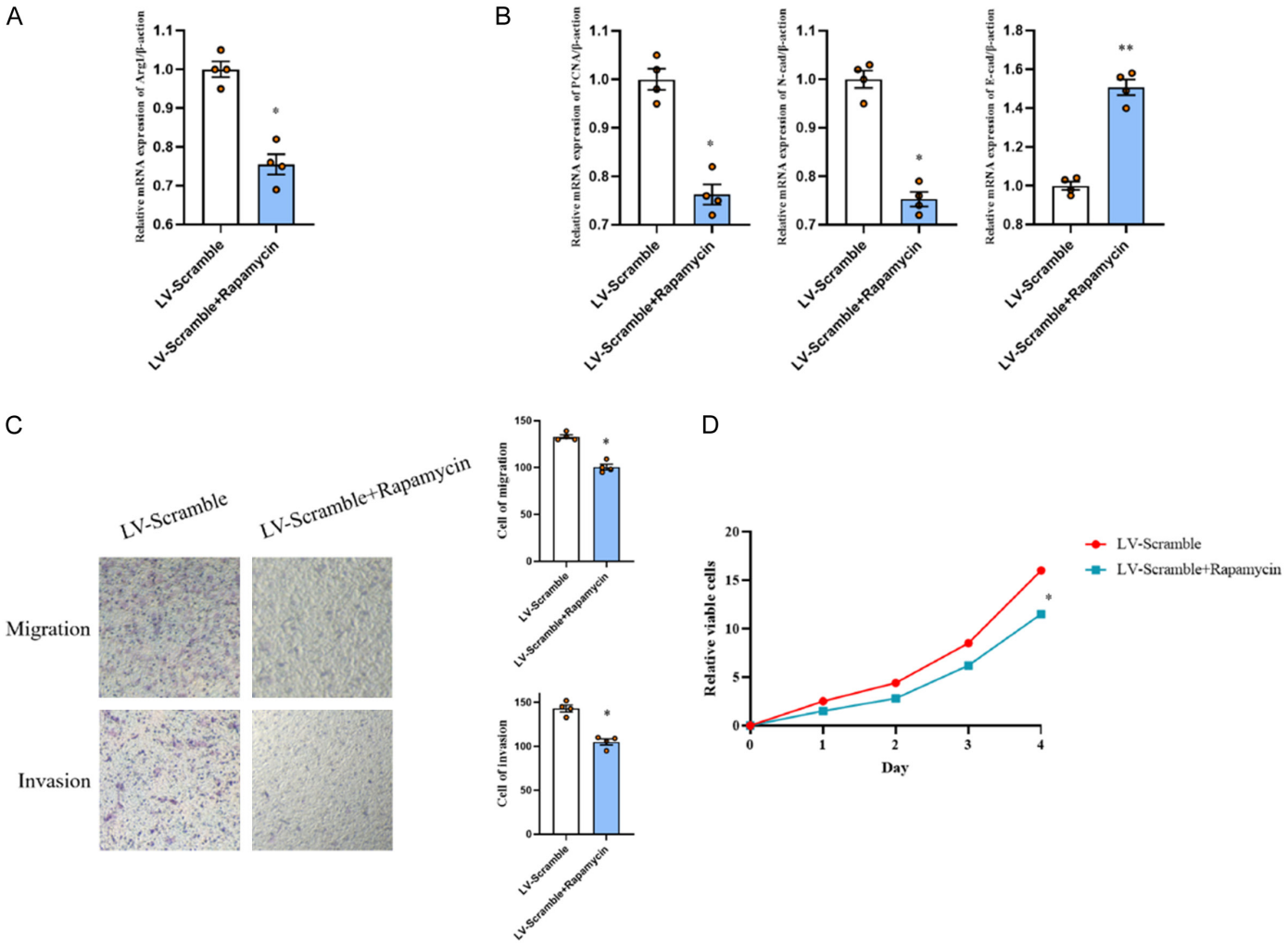
A
Relative mRNA expression of Arg1/β-action
LV-Scramble
LV-Scramble+Rapamycin
B
Relative mRNA expression of PCNA/β-action
Relative mRNA expression of N-cad/β-action
Relative mRNA expression of E-cad/β-action
C
LV-Scramble
LV-Scramble+Rapamycin
Migration
Invasion
Cell of migration
Cell of invasion
D
Relative viable cells
Day
LV-Scramble
LV-Scramble+Rapamycin

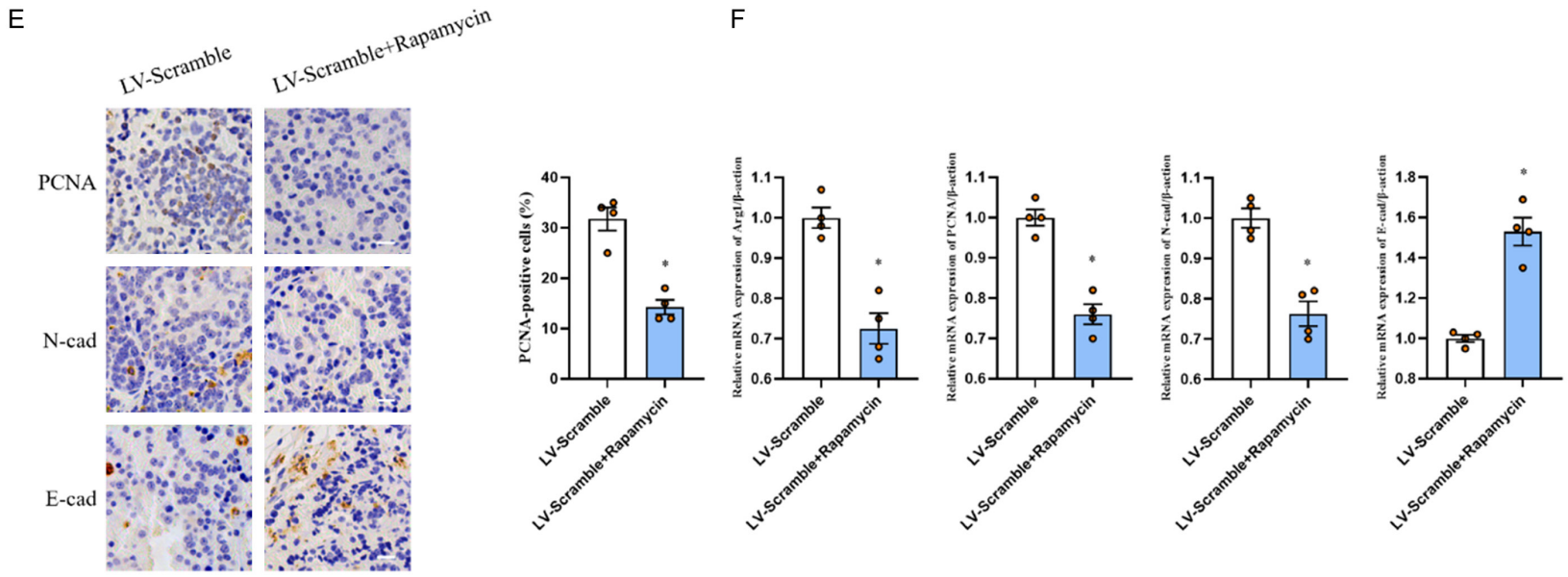

Figure S3. Rapamycin inhibits TAM polarization and glioma progression. A. mRNA expression of Arg1 (of groups LV-Scramble and LV-Scramble+Rapamycin; the same below) in BMDMs. B. mRNA expression of PCNA, N-cad, and E-cad in U251 cells. C. Transwell experiment evaluates the migration and invasion ability of tumor cells. D. CCK 8 experiment evaluates the proliferation ability of tumor cells. E. Immunohistochemistry was used to evaluate the expression of PCNA, N-cad, and E-cad in the tumor tissue (bar = 20 μm). F. mRNA expression of Arg1, PCNA, N-cad, and E-cad in the tumor tissue. *, $P < 0.05$; **, $P < 0.01$; ***, $P < 0.001$; ****, $P < 0.0001$, ns = no significance, compared with the group of LV-Scramble.